

Malignant Brain Tumor Detection

Amarjot Singh, Shivesh Bajpai, Srikrishna Karanam, Akash Choubey, and Thaluru Raviteja

Abstract—Brain tumor, a mass of tissue that grows out of control is one of the major causes for the increase in mortality among children and adults. Segmenting the regions of brain is the major challenge in tumor detection. A large number of effective segmentation algorithms have been used for segmentation in grey scale images ranging from simple edge-based methods to composite high-level approaches using modern and advanced pattern recognition approaches. Gradient vector field is an effective methodology applied to extract objects from complex backgrounds. The methodology has been effectively applied to extract different types of cancer like breast, skin, stomach etc. This paper uses a segmentation methodology called Gradient Vector Field, which uses energy as the feature to segment brain tumor along with a number of standard object detection algorithms mainly Sobel, Canny, Roberts, Prewitt and Laplacian. The performance of all the algorithms is tested on synthetic datasets followed by real MRI images. This paper (i) concludes the superiority of a particular methodology over others (ii) explains in detail the runtime analysis of the algorithms (iii) In depth analysis of the manual calculations of the parameters related to all the algorithms resulting into an optimized result with minimum error.

Index Terms—Tumor detection, gradient vector flow (GVF), active contour flow, sobel, canny, roberts, prewitt and laplacian.

I. INTRODUCTION

The current advancements in computer technologies have envisaged a developed vision based world, amended by artificial intelligence. This trend motivated the development in machine intelligence especially in the field of medical imaging. Medical imaging focuses to improve the real time medical image diagnosis. Since the development of medical imaging in clinical applications, a new era of unhurt diagnosis has evolved. Many techniques are being explored and practiced to improve clinical diagnosis. The main application is driven toward more generalized and significant application of medical imaging, related to a broader field of Brain tumor detection in MRI images. A tumor can be defined as a mass which grows without any control of normal forces [1]. Brain tumor detection is an important research area in terms of the association with the human life. The national brain tumor foundation (NBTF) for research in United States estimates the death of 13000 patients while 29,000 undergo primary brain tumor diagnosis. Brain tumor can be classified into two categories depending upon its

origin and growth. Brain tumor can be held responsible for mortality in children and adults.

Primary brain tumors are developed by brain cells covering the brain while secondary tumor is developed when cancer spreads to the brain from other parts of the body.

The segmentation of brain tissue and tumor in MRI images has been an active research area [2]. Segmenting specific regions of brain is considered to be the fundamental problem in image analysis related to tumor detection. A number of techniques have been used to segment MRI images. suchendra et al [3] proposed a multiscale image segmentation which uses a hierarchical self-organizing map for brain tumor segmentation [4]. It is a high speed parallel fuzzy c-mean algorithm. An improved implementation of brain tumor detection using segmentation based on neuro fuzzy technique [5] while chunyan et al. [6] designed a method on 3D variational segmentation for processes due to the high diversity in appearance of tumor tissue from various patients. Gradient vector field an extremely efficient algorithm has been used to segments objects in different environments [7]. It has been widely used to detect different types of cancers mainly skin cancer [8], breast cancer [9], stomach cancer [10] etc.

This paper focuses on the detection of brain tumor using gradient vector field, an energy based approach. GVF is tested on synthetic as well as real time MRI images and further is bench marked with the standard object detection algorithms mainly sobel, Canny, Roberts, Prewitt and laplacian. The algorithm interacts with local image features (edges, brightness), gradually deforming into the shape of the feature. The first type uses a generic active contour called snakes introduced by Kass *et al.* in 1987 [11]. Further need for accuracy, motivated the development of deformable templates [7] taking into account priori of features. The third version [12] termed as smart snakes is a generic flexible model which provides the best efficient interpretation of the brain tumor, possible by this method.

The remaining paper can be classified into following sections. Next section explains the GVF algorithm used to segment brain tumor. Section III presents a brief summary related to the standard operators. Section IV presents the results obtained by the algorithm on synthetic as well as real MRI databases. The results elaborate the extraction of brain tumor using GVF followed by the comparison with the standard operators. The section also explains in depth analysis of the manual calculations of the parameters related to all the algorithms resulting into an optimized result with minimum error. The last section elaborates the summary and conclusion in the respective field.

Manuscript received August 10, 2012; revised September 20, 2012.

A. Singh, S. Karanam, A. Choubey, and T. Raviteja are with the National Institute of Technology, Warangal, 506004 (e-mail: amarjotsingh@ieec.org).

S. Bajpai is with the Indian School of Mines Dhanbad, Jharkhand, India.

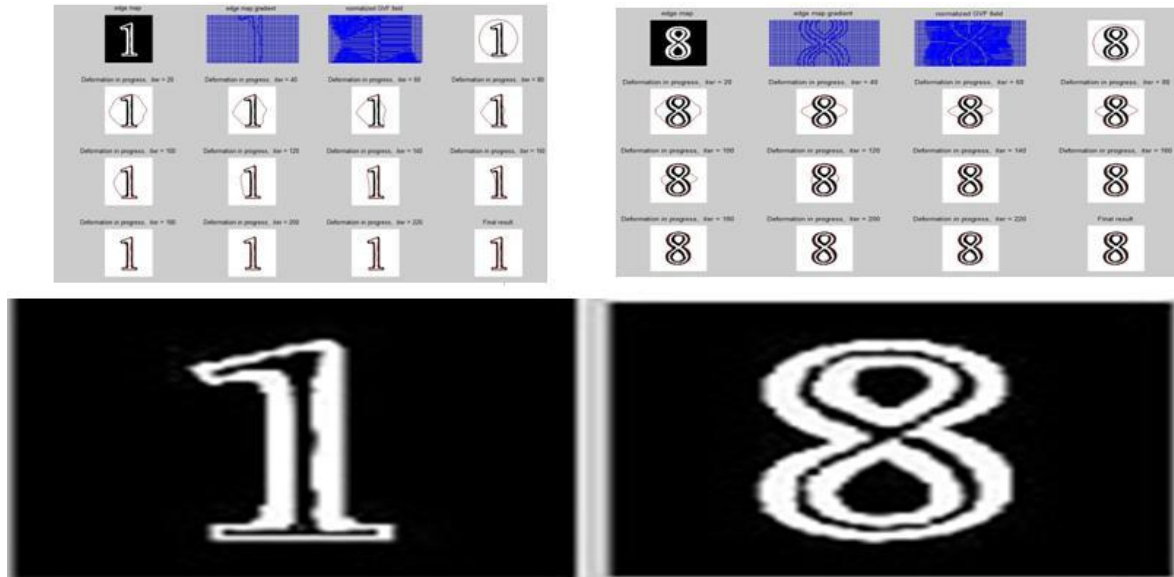


Fig. 1. (a) Simulations representing extraction with GVF applied on synthetic data of numbers 1 and 8 (b) Simulations representing extraction with standard edge operators sobel, canny, roberts, prewitt and laplacian applied on synthetic data of numbers 1 and 8.

II. ALGORITHMS

Unlike the previous described face detection techniques, this method aims to depict the actual high level appearance of features [13]. They are commonly used to locate head boundary or edges. The task is achieved by initializing the snake in the nearby proximity or region around the head. The snake gives the actual boundaries if released within approximate boundaries. The snake initialized converges onto the edges and subsequently assumes the shape of the head. The algorithm locks onto the features of interest which include mainly lines, edges or boundaries. The progress of traditional snake function $X(s)=[x(s),y(s)]$ for $s \in [0], [1]$ that moves through the spatial domain of an image $I(x, y)$ is obtained by minimizing the energy function

$$E_{energy} = \int_0^1 E_{energy}(X(s))ds \quad (1)$$

where E_{in} and E_{ext} are the internal and external energies respectively. Internal energy E_{in} is a combination of elasticity and strain energy defined as used to control the snake tension and rigidity, α represents elasticity while β describes the significance of stiffness term in snake's internal energy.

$$E_{in} = \frac{\alpha \left| \frac{dX(s)}{ds} \right|^2 + \beta \left| \frac{dX(s)}{ds} \right|^2}{2} \quad (2)$$

The external energies which force the snake towards the edge are elaborated as

$$E_{ext}(x, y) = |-\nabla I(x, y)|^2 \quad (3)$$

$$E_{ext}(x, y) = |-\nabla G_{\sigma}(x, y) * I(x, y)|^2 \quad (4)$$

where $G_{\sigma}(x, y)$ is a two dimensional Gaussian function with standard deviation σ and ∇ as the gradient operator. Minimization of energy provides the necessary energy required for the snake to shrink to the succeeding position. Finally, the snake reaches takes the shape of the head and the energy becomes zero. This intimates that the internal energy is equal to the force by image gradient. It is expressed as

$$E_{energy} = \alpha X'(s) - \beta X^{iv}(s) - \nabla E_{ext} = 0 \quad (5)$$

$F_{in} = \alpha X'(s) - \beta X^{iv}(s)$ is defined as the internal force that tries to stop the stretching and bending while $F_{ext} = \nabla E_{ext}$ is the external force that tries to pull the snake towards the desired image edge. After the force balance

$$F_{in} + F_{ext} = 0 \quad (6)$$

The initialization of the snake is a difficult task as we have to produce a suitable set of parameters as it is essential to for the initialization process. It is difficult to automatically generate the set of parameters for the objects of interest. Hence these constants are decided by the user. Once the parameters are decided correctly and the snake is released in the close proximity of the object, the face can be extracted successfully. It is an efficient method used in a number of applications requiring face detection.

III. EDGE DETECTION ALGORITHMS/OPERATORS

Many popular algorithms exist for edge detection. The basic aim of any edge detection algorithm is to locate the points in areas with high grey scale variations leading to the development of an edge between the two surfaces. Some of the edge detection algorithms are briefly discussed here.

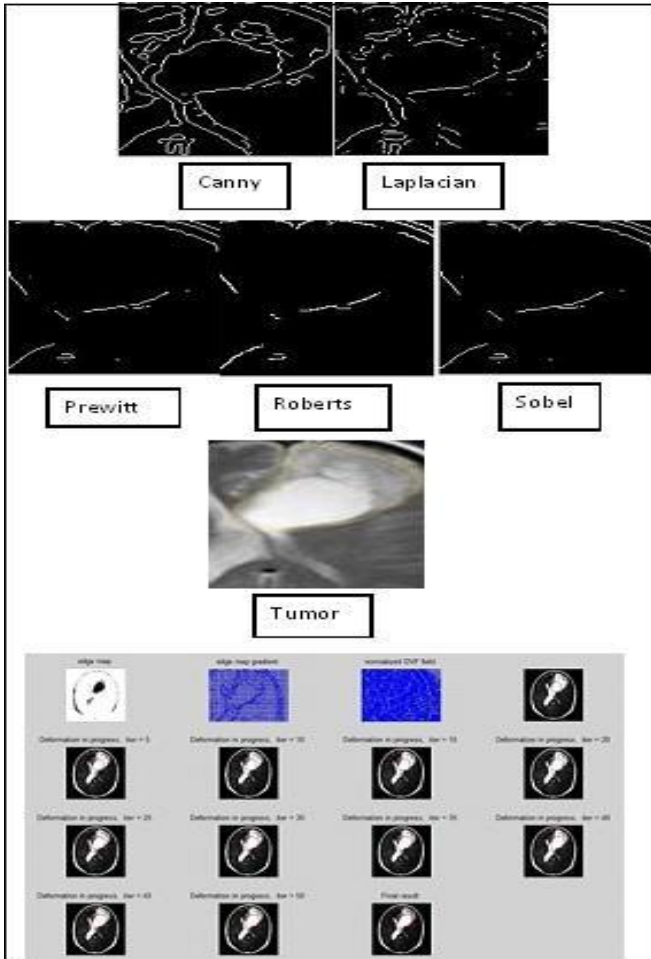


Fig. 2. (a) Extraction output for canny (b) extraction output for laplacian (c) extraction output for prewitt (d) extraction output for roberts (e) extraction output for sobel (f) tumor image (g) extraction with step by step convergence with GVF.

A. Canny Edge Detector

Canny [14] is an extremely famous and effective edge detector. Edge detection by the method involves a number of steps mainly (i) Noise removal (ii) Gradient computation (iii) Edge tracking. The raw image is convolved with a Gaussian filter resulting into in a slightly blurred version of the original image. The output from the convolution operation is not affected by noisy pixel to any significant degree. The next step involves the computation of intensity gradients returning a value for the first derivative in both horizontal and vertical directions. This information can be used to compute the gradient along with its direction.

$$|P| = \sqrt{(P_x)^2 + (P_y)^2}$$

Non-maximal suppression is applied to gradient magnitude to obtain a set of edge points in the form of a binary image. Double threshold is further used to extract the edges which were not visible using suppression. The edge pixels above the high threshold are marked as strong while the ones below the low threshold are suppressed. The edge pixels between the two are marked as weak. Strong edges are included in the final image and weak edges are included only if they are linked to strong edges. Strong edges are considered to be true edges while the weak edges are

included in the final output only if they are connected to the true edge as it can be generated by random noise. This method has been used over a number of years and has proved its worth in the field.

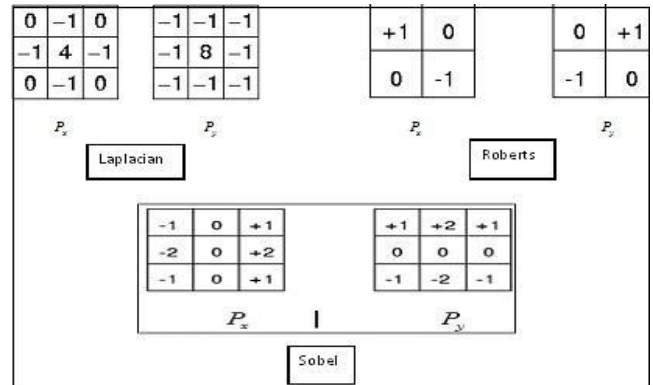


Fig. 3. Operators used for edge detection by (a) laplacian (b)roberts (c) sobel.

B. Sobel Operator

Sobel [15] is another operator used extensively for edge detection. The operator roughly computes the gradient of the function symbolizing the intensity of an image. The Sobel operator performs a 2-D spatial gradient measurement on the image underlining regions of high spatial frequency symbolizing the edges. The operator makes use of a pair of 3x3 convolution kernels are shown in Fig. 3(c). These kernels are convolved with the source image to evaluate the derivatives in both horizontal and vertical directions. The derivatives are further used to compute the absolute magnitude of the gradient at each point of the image is given by:

$$|P| = \sqrt{(P_x)^2 + (P_y)^2}$$

The direction of the gradient is given by

$$\alpha = \arctan\left(\frac{P_y}{P_x}\right)$$

The convolution kernels of the Sobel edge detector are larger due to which the input image is smoothed to a larger extent, thus making it less sensitive to noise. The Sobel operator makes use of this point in detecting edges by comparing the gradient value at a particular pixel with a predefined threshold value, and if it exceeds the threshold, it is included as an edge location.

C. Roberts Edge Operator

The Robert Cross [16] operator performs a 2-D spatial gradient measurement on a source image resulting into the regions of high spatial frequency corresponding to edges. This operator makes use of a pair of 2x2 convolution kernels as shown in Fig. 3(b). The source image is convolved with the presented kernels, resulting in both horizontal and vertical gradients. The absolute magnitude of gradient at a point is evaluated by:

$$|P| = \sqrt{(P_x)^2 + (P_y)^2}$$

The direction of the gradient is given by:

$$\alpha = \arctan\left(\frac{P_y}{P_x}\right)$$

The advantage of the Roberts edge detector is that it works quite fast because of its small size. However it is irrisistent to noise and also fails in detecting very sharp edges. The sobel operator makes use of this point in detecting edges by comparing the gradient value at a particular pixel with a predefined threshold value, and if it exceeds the threshold, it is concluded as an edge location.

D. Prewitt Edge Operator

Prewitt [17] is another operator used for edge detection and extraction. This operator calculates the maximum response for a set of convolution kernels and finds the orientation of edges for each pixel of the image under consideration. In most of the edge detection techniques finding the magnitude of orientation of the edges in x and y directions is tedious. The Prewitt edge detector overcomes this problem by finding the orientation straightforward from the kernels with the maximum response. The sobel operator makes use of this point in detecting edges by comparing the gradient value at a particular pixel with a predefined threshold value, and if it exceeds the threshold, it is concluded as an edge location. The Prewitt edge detector otherwise doesn't differ much from the Sobel operator.

E. Laplacian of Gaussian

This edge detector [18] extracts the edge by using a combination of Gaussian filtering and laplacian operator. In first step, the noise in an image is decreased by convoluting the particular image with a Gaussian filter resulting into the filtering of the all the noisy points out of the image. In the next step, gradient is measured for the image being analysed by detecting the zero-crossings of the second order difference of the image resulting into edges. The image is first smoothed by convolution with a Gaussian kernel of width σ to filter out all the noise present in the image given by:

$$G_\sigma(x, y) = \frac{1}{\sqrt{2\pi\sigma^2}} e^{\left[\frac{-(x^2+y^2)}{2\sigma^2}\right]}$$

The laplacian of the image whose intensity values are represented as $f(x, y)$ is defined as

$$L(x, y) = \frac{\partial^2 f}{\partial x^2} + \frac{\partial^2 f}{\partial y^2}$$

Since the input image is shown as having discrete pixels, we need to approximate the second derivatives in the equation for laplacian operator for which either of the shown convolution kernels can be used. As the convolution operation is associative, the Gaussian filter can be convolved with the laplacian filter and then the hybrid filter can be convolved with the image to get the results.

IV. RESULTS

The results obtained from the simulations enable us to investigate the capability of the method applied to synthetic and real time datasets. The algorithm is simulated on a Pentium core 2 duo 1.83 GHz machine. This section presents the extraction results for one and eight, presented as synthetic data while real MRI image of malignant brain tumor dataset. The section also computes and compares the runtime analysis and the accuracy of tumor detected, compared across a common ground truth for GVF method across all standard methodologies. The algorithms are compared on the basis of error incurred during extraction as well as runtime analysis. The section also focuses on the manual computation of the parameters used in the algorithm.

The algorithms are primarily tested on synthetic dataset as shown in Fig. 1 (a). The algorithms are applied to extract two numbers, one and eight mentioned above as synthetic dataset inputs. The simulation results obtained for active contour method applied to synthetic dataset has been shown in Fig. 1 (a). The results show the edge map and GVF normalized field followed by the step by step deformation of the snake, which finally encloses the boundary of the object. The method successfully detected and finally extracted the numbers as described above. The whole process computes in 2 second with 220 iterations. As, the parameter have to adjusted manually, the accuracy mainly depends upon the selection of the parameters. The output for the edge operators applied to the synthetic dataset has been shown in Fig. 1 (b). Error in the output is defined as the total number of pixels unclassified in the region of interest over the total number of pixels in the region of interest. The number of iterations is a prime factor for snake regularization. The maximum error of 8.02 is incurred for 60 iterations while the minimum error of 7.17 is obtained for 130 iterations. Another important parameter which affects the performance of snake is the initialization distance between the two points. The maximum error in the output is 8.08 for a maximum distance (DMAX) of 1.75 and minimum error is 6.9 for a maximum distance (DMAX) of 4.5 between initialization points. Similarly, maximum error of 7.25 is observed for a minimum distance (DMIN) of 0.25 and a minimum error of 6.9 for a minimum distance (DMIN) of 1 between initialization points. The elasticity parameter alpha plays an important role in governing the shape of the snake. The error varies from a maximum value of 8.16 for alpha equal to 0.05 to 6.9 for, 0.5 alpha value. Using the optimum values of the parameters, we obtain a minimum error of 4.6%. The error incurred by the standard operators sobel, Canny, Roberts, Prewitt and laplacian is almost equal to zero. Hence the operators are perfectly able to detect the number due to the high grayscale variation between the background and the numbers.

In the next step the algorithm is tested on 5 malignant brain tumor MRI images with the FOV by measuring SNR and SDNR values at a FOV of 20cm, 28cm 36cm, and 42cm as shown in Fig. 2 (f). Fig. 2(g) shows the edge map gradient and GVF field obtained during the simulations followed by the step by step evolution of the snake which finally encloses and captures the tumor. The method effectively extracts the tumor in 50 iterations. The method takes 14 seconds for the whole process. The error approach could not be extracted on

the original tumor image owing to the small size of tumor. The error variations on varying the parameters are not significant. In order to compare the effectiveness of the algorithm, all the standard operators are applied to the tumor image. It is observed that none of the standard edge operator is able to extract the tumor from the image as shown in Fig. 2(a-e) canny and laplacian identifies maximum number of edges. On the other hand, the inability of the remaining edge operators prewitt, roberts and sobel is clearly evident in Fig. 2 (c-e). The operators were incapable of identifying the tumor as the output includes muscles have similar gray scale as of tumor.

V. CONCLUSION

The level set method offer a powerful approach for image segmentation among the various image segmentation techniques due to its ability to handle any of the cavities, concavities, splitting/merging and convolution. The above mentioned method has huge potential in a non-trivial domain involving small segmentation parameters and compromised efficiency. On the other hand, edge operator identifies objects on the basis of grayscale variations between the object and background. In case tumor in the image, the tumor is on muscles having very similar grayscale variation resulting into inability of the edge operators to extract the tumor. On the other hand, GVF works on the principle of energy minimization hence effectively extracting the tumor. The parameters of GVF has to be controlled manually which is time consuming process and may lead to error in the results. Overall, GVF gives better results when applied to images in controlled background.

REFERENCES

- [1] N. R. Pal and S. K. Pal, "A review on image segmentation techniques," *Pattern Recognition*, vol. 26, no. 9, pp. 1277-1294, 1993
- [2] L. P. Clarke, R. P. Velthuizen, M. A. Camacho, J. J. Heine, M. aidyanathan, L. O. Hall, R. W. Thatcher, and M. L. Silbiger, "MRI segmentation: methods and applications," *Magn Reson Imaging*, vol. 13, no. 3, pp. 343-68, 1995.
- [3] M. B. Suchendra, K. B. Jean, and S. B. Minsoo, "Multiscale image segmentation using a hierarchical self-organizing map," *Neurocomputing*, vol. 14, pp. 241-272, 1997
- [4] S. Murugavalli and V. Rajamani, "A high speed parallel fuzzy cmean algorithm for brain tumor segmentation," *BIME Journal*, vol. 6, 2006
- [5] S. Murugavalli and V. Rajamani, "An improved implementation of brain tumor detection using segmentation based on neuro fuzzy technique," *J. Comp. Sc.* vol. 3, no. 11, pp. 841-846, 2007.
- [6] J. Chunyan, Z. Xinhua, H. Wanjun, and M. Christoph, "Segmentation and quantification of brain tumor," *IEEE International Conference on Virtual Environment, Human-Computer Interfaces and Measurement Systems*, USA, pp. 12-14, 2004.
- [7] L. Yuille, P. W. Hallinan, and D. S. Cohen, "Features extraction from faces using deformable templates," *International Journal of Computer*, vol. 8, pp. 99-111, 1992.
- [8] J. Tang, "A multi-direction GVF snake for the segmentation of skin cancer images," *Pattern Recognition*, vol. 42, no. 6, pp. 1172-1179, June 2009.
- [9] F. Zou, Y. Zheng, Z. Zhou, and K. Agyepong, "Gradient vector flow field and mass region extraction in digital mammograms," *International Symposium Computer-Based Medical Systems*, pp. 41-43, June 2008.
- [10] H. Zhang and G. Li, "Application in stomach epidermis tumors segmentation by GVF snake model," *International Seminar on Future BioMedical Information Engineering*, pp. 453-456, 2008.
- [11] M. Kass, A. Witkin, and D. Trezopoulos, "Snakes: Active contour models," *International Journal of Computer Vision*, vol. 1, no. 4, pp. 321-331, 1987.
- [12] T. F. Cootes and C. J. Taylor, "Active shape models-smart snakes," in *Proceedings of British Machine Vision Conference*, pp. 266-275, 1992.
- [13] C. Xu and J. L. Prince, "Snakes, shapes and gradient vector flow," *IEEE Transaction on Image Processing*, vol. 7, no. 3 pp. 359-369, March 1998.
- [14] J. Canny, "A computational approach to edge detection," *IEEE Transactions on Pattern Analysis and Machine Intelligence*, vol. 8, no. 6, Nov. 1986
- [15] L. Sobel, *Camera Models and Machine Perception*, PhD dissertation, Stanford University Artificial Intelligence Lab, Stanford University, CA, 1970.
- [16] L. G. Roberts, "Machine perception of three-dimensional solids," *Optical and Electro-Optical Information Processing*, J. T. Tippet et. al., Eds. Cambridge, MA, MIT Press, 1965.
- [17] J. Prewitt, "Object enhancement and extraction," *Picture Process Psychopict*, pp. 75-149, 1970.
- [18] D. Marr and E. Hildreth, "Theory of edge detection," *Proc. Roy. Soc., London*, vol. 207, pp. 187-217, 1980.